Excitation of backward waves in forward wave amplifiers

G. S. Nusinovich, M. Walter, and J. Zhao
Institute for Plasma Research, University of Maryland, College Park, Maryland 20742-3511
(Received 15 May 1998)

The sources of coherent electromagnetic radiation based on amplification of traveling waves by electron beams have unique capabilities of wide band, high efficiency operation. The most critical issue in the development of such forward wave amplifiers is the self-excitation of parasitic backward waves in the interaction region. The developed theory allows one to analyze the nonlinear effect of suppression of parasitic backward waves by forward waves operating in the large-signal regime. The results of the analysis of traveling wave tubes (TWTs) and twystrons driven by linear electron beams and the results of the study of gyrodevices (gyro-TWTs and gyrotwystrons) driven by beams of gyrating electrons are presented. The gyrodevices are considered in the cases when the forward and backward waves are in resonance with electrons either at the first or second cyclotron harmonic. The results obtained allow one to estimate to what extent the coupling of an electron beam to the parasitic wave should be decreased in order to provide a stable, high efficiency amplification of the forward wave. [S1063-651X(98)14011-4]

PACS number(s): 52.75.Ms, 84.40.Ik, 84.40.Fe

I. INTRODUCTION

Traveling wave amplifiers (TWAs) based on amplification of electromagnetic (EM) waves by electron beams are of importance for many applications, including communication systems, since the bandwidth of TWAs is typically much larger than that of other sources of radiation. In order to combine this large bandwidth with a high gain in TWAs, it is necessary to have a long enough interaction region.

The main obstacle in realizing such large-bandwidth, high-gain amplifiers is the excitation of parasitic backward waves in long waveguides where the forward waves are amplified. This problem is extremely important for the sources of coherent Cherenkov, or Smith-Purcell, EM radiation driven by linear electron beams, e.g., traveling wave tubes (TWTs) and twystrons (see, e.g., Ref. [1]), as well as for the sources of bremsstrahlung radiation, which are driven by beams of oscillating electrons. The most advanced classes of such devices are cyclotron resonance masers (CRMs) [2] and free electron lasers (FELs) [3]. Among traveling wave configurations of CRMs, the best known are gyro-traveling wave tubes (gyro-TWTs) and gyrotwystrons (see, e.g., Ref. [4]). Similar configurations are also known for FELs.

Several methods are usually used for providing the stability of efficient operation in traveling waves. Some of these methods can be characterized by introducing lossy materials (see, e.g., Ref. [5], and references therein) or severs, which transform a single stage device into a two or more stage configuration (see Ref. [6], and references therein). Note that, as shown in Ref. [7], distributed wall losses are a more effective means for suppressing parasitic instabilities than severs.

Another method of preventing spurious excitation of backward waves is nonlinear suppression [8], which is based on the nonlinear effects in an electron beam caused by the presence of the forward wave. (The effect of nonlinear suppression of unwanted modes in gyrotron oscillators was analyzed in Refs. [9] and [10].) Nonlinear interaction between forward and parasitic backward waves was studied by different methods in Refs. [11] and [6] for some specific sets of parameters. The results of these simulations agreed well with experimental data. A more general approach based on the Hamiltonian formalism was developed in Ref. [12]. This formalism allows one to study the excitation of forward waves and the stability of operation with respect to parasitic modes in gyro-traveling wave devices driven by relativistic electron beams when the waveguide and external magnetic field profiles can be slightly tapered and the wave reflection from the output is possible. Based on this formalism the analysis of the relativistic 10 GHz, 430 kV, 240 A gyrotwystron was done. However, the large number of factors taken into account did not allow the authors to analyze in Ref. [12] some general tendencies in the suppression of backward waves by forward waves operating in the large signal regime. This is the topic of our paper.

The paper is organized as follows. Section II contains the formalism describing the excitation of small-amplitude backward waves in the presence of large amplitude forward waves in gyro-traveling-wave amplifiers. In the limiting case of dominant inertial orbital bunching of electrons, these equations are reduced to equations describing the excitation of backward waves in TWTs driven by linear electron beams. (Note that the same equations are valid for FELs and other sources of coherent radiation that, under certain assumptions, can be described by TWT equations [13].) Section III contains the results of our study of the simplest equations in the case of two configurations: the first is a traveling wave configuration in which at the entrance an electron beam is not prebunched and the input forward wave has a small but nonzero amplitude; the second is an output waveguide of a twystron in which at the entrance the prebunched electron beam starts to excite a forward wave with a zero initial amplitude. Section IV contains the results of similar analysis of self-excitation conditions of backward waves in gyro-TWTs and gyrotwystrons, including the cases when backward and forward waves interact with electrons at either the fundamental or second cyclotron harmonic. The cases of simultaneous interaction at different harmonics (e.g., the backward wave at the fundamental harmonic and the forward wave at the second harmonic, or vice versa) are also analyzed. Section V contains a discussion of these results, and in Sec. VI we make our conclusions. The derivation of equations describing the excitation of backward waves in the presence of forward waves is given in the Appendix.

II. GENERAL EQUATIONS

Bearing in mind that, as mentioned in the Introduction, the equations for gyro-TWAs can be reduced [14], in the regime of dominant orbital bunching, to the equations for TWAs driven by linear electron beams, we will start with a consideration of gyro-TWAs. Let us represent the electric field of two waves as

$$\mathbf{E}=\mathrm{Re}\{A_1(z)\mathbf{E}_1(\mathbf{r}_\perp)e^{i(\omega_1 t-k_{1,z}z)}+A_2(z)\mathbf{E}_2(\mathbf{r}_\perp)e^{i(\omega_2 t+k_{2,z}z)}\}, \tag{1}$$

where A_1 and A_2 are the amplitudes of, respectively, the forward and backward waves, which slowly vary along the axis ($|dA/dz|\ll k_z A$) in the process of interaction with electrons, functions $\mathbf{E}_1(\mathbf{r}_\perp)$ and $\mathbf{E}_2(\mathbf{r}_\perp)$ describe the transverse structure of the waves, and $\omega_{1,2}$ and $k_{1,2,z}$ are, respectively, their frequencies and axial wave numbers. The equation of motion for a relativistic electron moving in the external constant magnetic field, $\mathbf{H}_0=H_0\mathbf{z}_0$, and the electromagnetic field of two waves can be written as

$$\frac{d\mathbf{p}'}{dz'}+\gamma_0\left[\frac{\mathbf{p}'}{p_z'}\times\mathbf{z}_0\right]=-\frac{1}{\beta_z}\{\mathbf{E}'+[\boldsymbol{\beta}\times\mathbf{H}']\}. \tag{2}$$

Here the electron momentum is normalized to m_0c, $\mathbf{p}'=\mathbf{p}/m_0c$, $z'=\Omega_0 z/c$ is the normalized axial coordinate (Ω_0 is the unperturbed electron cyclotron frequency), $\boldsymbol{\beta}$ is the electron velocity normalized to the speed of light, c, and the electric and magnetic fields ($\mathbf{E}'$ and $\mathbf{H}'$, respectively) of the two waves are normalized to $m_0c\Omega_0/e(A'=eA/m_0c\Omega_0)$.

A. Amplification of the forward wave

Since our goal is to study only the self-excitation of backward waves, we will assume that the amplitude of the backward wave A_2 is much smaller than the amplitude of the forward wave A_1. In the limiting case $A_2\to 0$ Eq. (2) and the equation for the forward wave excitation, which follows from the Maxwell equations, can be reduced, as described elsewhere [15–17], to a self-consistent set of equations describing the stationary operation of gyro-TWAs:

$$\frac{du}{dz'}=-2\frac{(1-u)^{s_1/2}}{1-b_1u}\,\mathrm{Re}(F_1e^{-i\theta}), \tag{3}$$

$$\frac{d\theta}{dz'}=\frac{1}{1-b_1u}\{\mu_1u-\Delta_1+s_1(1-u)^{(s_1/2)-1}\,\mathrm{Im}(F_1e^{-i\theta})\}, \tag{4}$$

$$\frac{dF_1}{dz'}=-I_1\frac{1}{2\pi}\int_0^{2\pi}\frac{(1-u)^{s_1/2}}{1-b_1u}e^{i\theta}d\theta_0. \tag{5}$$

Here the variable

$$u=2\frac{1-h_1\beta_{z0}}{\beta_{\perp 0}^2}\frac{\gamma_0-\gamma}{\gamma_0}$$

describes the variation in electron energy $\mathcal{E}$ ($\gamma=\mathcal{E}/m_0c^2$ is the electron energy normalized to the rest energy and h_1 is the axial wave number $k_{1,z}$ normalized to ω_1/c); the parameter $b_1=h_1\beta_{\perp 0}^2/2\beta_{z0}(1-h_1\beta_{z0})$ is responsible for the recoil effect (i.e., the changes in the electron axial velocity in the process of radiation of electromagnetic waves); F_1 is the normalized forward wave amplitude [15–17], and

$$\theta=s_1\Theta-(\omega_1t-k_{1,z}z)-\varphi_1 \tag{6}$$

is the slowly variable phase of the resonant harmonic of electron gyrations with respect to the phase of the forward wave. The cyclotron resonance condition for the forward wave has the form

$$|\omega_1-k_{1,z}v_{z0}-s_1\Omega_0|\ll\Omega_0;$$

in Eqs. (3)–(5) the resonant harmonic number s as well as other parameters are related to the forward wave. The phase φ_1 in Eq. (6) is determined by the transverse structure of the wave in the vicinity of the guiding center of a gyrating electron. As shown in Ref. [18] (see also Refs. [16] and [17]), this structure can be described by the function

$$L_1=\left[\frac{1}{k_{1,\perp}}\left(\frac{\partial}{\partial X}+i\frac{\partial}{\partial Y}\right)\right]^{s_1}\Psi(X,Y), \tag{7}$$

which we represented as $|L_1|e^{i\varphi_1}$. In Eq. (7), $k_{1,\perp}$ is the transverse wave number, X and Y are transverse coordinates of the guiding center, the function Ψ is the membrane function which obeys the Helmholtz equation with the corresponding boundary condition for the $\mathrm{TE}_{m,p}$ wave at the waveguide wall. In cylindrical waveguides $L=J_{m\mp s_1}(k_{1,\perp}R_0)e^{-i(m-s_1)\psi}$, where R_0 and ψ are, respectively, the radial and azimuthal coordinates of the guiding center [so $\varphi_1=-(m-s_1)\psi$]. Also in Eq. (4), the parameter

$$\mu_1=\frac{s_1(1-h_1^2)\beta_{\perp 0}^2}{2\beta_{z0}(1-h_1\beta_{z0})^2} \tag{8}$$

describes the changes in the gyrophase with respect to the wave in the process of interaction and

$$\Delta_1=\frac{s_1}{1-h_1\beta_{z0}}\frac{1}{\beta_{z0}}\left(1-h_1\beta_{z0}-s_1\frac{\Omega_0}{\omega_1}\right) \tag{9}$$

is the normalized initial mismatch of the cyclotron resonance. In Eq. (5) I_1 is the normalized beam current parameter,

$$I_1=4\frac{eI_b}{m_0c^3}\frac{(\kappa_1s_1)^{2s_1}}{h_1}\frac{\beta_{\perp 0}^{2(s_1-1)}}{\gamma_0\beta_{z0}^2(1-h_1\beta_{z0})^{2s_1-1}}\times\left[\frac{1}{(s_1-1)!2^{s_1}}\right]^2G, \tag{10}$$

where the coupling parameter G for a cylindrical waveguide with a thin annular electron beam is equal to

$$G=\frac{J^2_{m\mp s_1}(k_{1\perp}R_0)}{(\nu^2-m^2)J^2_m(\nu)}. \tag{11}$$

Here, $\nu=k_{1\perp}R_w$ is the pth root of the equation $J'_m(\nu)=0$, which is the boundary condition for the $\mathrm{TE}_{m,p}$ wave at the waveguide wall of radius R_w; κ in Eq. (10) is the transverse wave number normalized to ω/c.

Boundary conditions for Eqs. (3)–(5) depend on the configuration of the device. At the entrance to the gyro-TWT's interaction region, at $z'=0$, $u=0$, $\theta=\theta_0$ (where θ_0 is homogeneously distributed from 0 to 2π) and $F=F_0$ (where F_0 is the input wave amplitude). At the entrance to the output waveguide of the gyrotwystron, the energy modulation can be negligibly small ($u\simeq 0$), but the phase bunching is significant: $\theta(0)=\theta_0-q\sin\theta_0$. The latter boundary condition is given for the simplest, one-cavity prebunching case; θ_0 is here the entrance phase for the input cavity and the bunching parameter q is proportional to the amplitude of the input cavity field multiplied by the drift section length. (Boundary conditions for more complicated schemes are given elsewhere [19].) This prebunched electron beam excites in the output waveguide a wave with a zero amplitude at the entrance: $F(0)=0$. (The latter implies the absence of reflections from a well matched output of this waveguide.)

B. Excitation of backward waves

As mentioned above, we will assume that the amplitude of the parasitic backward wave is much smaller than the amplitude of the operating forward wave. This allows us to treat the effect of the backward wave on electrons as small perturbations in electron motion. Under these assumptions the excitation of backward waves in gyro-TWAs, as shown in the Appendix, can be described by the following equations:

$$\frac{d\overline{p_\perp}}{d\zeta'}=\frac{1}{2}(1-u)^{(s_2-1)/2}F'_2e^{-i\bar{\bar{\theta}}}, \tag{12}$$

$$\frac{d\overline{\theta}}{d\zeta'}=-2s_2(1-u)^{1/2}\overline{p_\perp}-i\,\frac{s_2}{2}(1-u)^{(s_2/2)-1}F'_2e^{-i\bar{\bar{\theta}}}, \tag{13}$$

$$\frac{dF'_2}{d\zeta'}-i\Delta'_2F'_2=I'_2\,\frac{1}{2\pi}\int_0^{2\pi}(1-u)^{s_2/2}e^{i\bar{\bar{\theta}}}\times\left\{\frac{s_2}{\sqrt{1-u}}\,\overline{p}_\perp+i\overline{\theta}\right\}d\theta_0. \tag{14}$$

These equations are valid when both the forward and backward waves are excited at frequencies close to cutoff. (They are given in a more general form in the Appendix.) Here the normalized axial coordinate is $\zeta'=(\beta^2_{\perp 0}/2\beta_{z0})z'$,

$$\Delta'_2=\frac{2\beta_{z0}}{\beta^2_{\perp 0}}\,\Delta_2=\frac{2s_2}{\beta^2_{\perp 0}}\left(1+h_2\beta_{z0}-s_2\,\frac{\Omega_0}{\omega_2}\right).$$

Variables $\overline{p}_\perp$ and $\overline{\theta}$ in Eqs. (12)–(14) are perturbations in, respectively, the orbital momentum and gyrophase, averaged over the phase difference $\overline{\psi}$. In the case when azimuthal indices of both waves, m_1 and m_2, obey the condition [20] $s_1m_2\neq s_2m_1$, this corresponds to the averaging over electron distribution in azimuthal coordinates of guiding centers (see Appendix for details). The phase $\bar{\bar{\theta}}$ in Eqs. (12)–(14) relates to the phase θ determined by Eq. (4) as

$$\bar{\bar{\theta}}=\frac{s_2}{s_1}(\theta+\Delta_1z').$$

So, the equation for $\bar{\bar{\theta}}$ can be written as

$$\frac{d\bar{\bar{\theta}}}{d\zeta'}=s_2u+s_2(1-u)^{(s_1/2)-1}\,\mathrm{Im}(F'_1e^{-i\theta_1}), \tag{15}$$

where

$$\theta_1=\theta+\Delta'_1\zeta',\quad F'_1=\frac{2\beta_{z0}}{\beta^2_{\perp 0}}\,F_1e^{i\Delta'_1\zeta'},$$

$$\Delta'_1=\frac{2\beta_{z0}}{\beta^2_{\perp 0}}\,\Delta_1=\frac{2s_1}{\beta^2_{\perp 0}}\left(1-h_1\beta_{z0}-s_1\,\frac{\Omega_0}{\omega_1}\right).$$

The self-consistent set of equations (3)–(5) describing the forward interaction can be rewritten in these variables as

$$\frac{du}{d\zeta'}=-2(1-u)^{s_1/2}\,\mathrm{Re}(F'_1e^{-i\theta_1}), \tag{16}$$

$$\frac{d\theta_1}{d\zeta'}=s_1u+s_1(1-u)^{(s_1/2)-1}\,\mathrm{Im}(F'_1e^{-i\theta_1}), \tag{17}$$

$$\frac{dF'_1}{d\zeta'}-i\Delta'_1F'_1=-I'_1\,\frac{1}{2\pi}\int_0^{2\pi}(1-u)^{s_1/2}e^{i\theta_1}d\theta_0. \tag{18}$$

Here,

$$I'_1=\left(\frac{2\beta_{z0}}{\beta_{\perp 0}}\right)^2I_1.$$

The parameter I'_2 in Eq. (14) relates to I_2 determined by Eq. (10), after corresponding changes in indices, in the same way as I'_1 relates to I_1.

The self-consistent set of equations (16)–(18) has the integral

$$|F'_1|^2-|F'_0|^2=I'_1\,\frac{1}{2\pi}\int_0^{2\pi}u\,d\theta_0, \tag{19}$$

which corresponds to the energy conservation law. Taking into account the definition of u, one can show that the value

$$\eta_\perp=\frac{1}{2\pi}\int_0^{2\pi}u\,d\theta_0 \tag{20}$$

in the right-hand side of Eq. (19), which is known as the orbital efficiency (see, e.g., Refs. [14–17]), relates to the total electron efficiency η as

$$\eta=\frac{\beta^2_{\perp 0}}{2(1-\gamma_0^{-1})(1-h_1\beta_{z0})}\,\eta_\perp. \tag{21}$$

So, Eq. (19) can be rewritten as

$$|F_1'|^2-|F_0'|^2=I_1'\eta_\perp, \tag{22}$$

where the input wave amplitude F_0' in gyrotwystrons is equal to zero and in high-gain gyro-TWTs is negligibly small.

So, first, Eqs. (16)–(18), describing the large-signal forward wave interaction, should be solved together with Eq. (15), which determines the phase $\bar{\bar{\theta}}$ present in Eqs. (12)–(14), and with Eq. (20), which determines the efficiency. Then, this solution should be used in Eqs. (12)–(14), describing the excitation of the backward wave in the small-signal regime.

In the absence of the forward wave in Eqs. (12)–(14), $u=0$ and $\bar{\bar{\theta}}=\bar{\bar{\theta}}(0)-\Delta_2'\zeta'$. So, introducing $\hat{F}_2=F_2'e^{i\Delta_2'\zeta'}$, $\hat{p}=(1/2\pi)\int_0^{2\pi}\overline{p}e^{i\theta_0}d\theta_0$, $\theta=(1/2\pi)\int_0^{2\pi}\overline{\theta}e^{i\theta_0}d\theta_0$ (assuming a nonprebunched beam at the entrance) we can reduce Eqs. (12)–(14) to

$$\frac{d\hat{p}}{d\zeta'}=\frac{1}{2}\hat{F},$$

$$\frac{d\hat{\theta}}{d\zeta'}=-\frac{s_2}{2}(\hat{p}+i\hat{F}),$$

$$\frac{d\hat{F}}{d\zeta'}-i\Delta_2'\hat{F}=I_2'(s_2\hat{p}+i\hat{\theta}).$$

For perturbations $\sim e^{i\delta\zeta'}$, these equations yield the dispersion equation (cf. Refs. [14] and [15])

$$(\delta-\Delta_2')\delta^2+I\delta-I=0, \tag{23}$$

in which $I=s_2I_2'$. At small values of I one can introduce $\hat{\delta}=\delta/I^{1/3}$, $\hat{\Delta}=\Delta_2'/I^{1/3}$, and, neglecting small terms, reduce Eq. (23) to the dispersion equation

$$(\hat{\delta}-\hat{\Delta})\hat{\delta}^2-1=0, \tag{24}$$

well known in the theory of conventional backward oscillators [21]. As is known, the starting conditions, which follow from solving Eq. (24) together with the boundary conditions for a nonprebunched beam at the entrance and for the backward wave at the well-matched output [the latter is $\hat{F}(L)=0$, where $L=I^{1/3}\zeta_{\rm out}'$ is the normalized length of the interaction region], yield $L=1.97$ and $\hat{\delta}=1.522$. Note that for a waveguide with Ohmic losses in the walls, the axial wave number h_2 in the detuning $\hat{\Delta}$ is complex; also any tapering of the waveguide radius and losses can be described by the corresponding dependence of $\hat{\Delta}$ on the axial coordinate.

C. Dominant inertial bunching

The regime of the dominant inertial orbital bunching mentioned in the Introduction implies a small value of the normalized beam current parameter I_1 when the wave amplitude is small and efficient orbital electron bunching under the action of this wave requires a long interaction region. In this regime the changes in electron energy are small since we can estimate them, as follows from Eq. (3), as $|u|\sim F_1z'\ll 1$. However, the phase bunching caused by these changes can be large, since the first term in the right-hand side of Eq. (4) leads to the phase changes on the order of $\mu F_1(z')^2\sim\pi$. So, in comparison with this term, the last term in the right-hand side of Eq. (4), which is on the order of F_1z', can be neglected. In this approximation, Eqs. (3)–(5) are reduced to

$$\frac{du}{dz'}=-2\,\mathrm{Re}(F_1e^{-i\theta}), \tag{25}$$

$$\frac{d\theta}{dz'}=\mu_1u-\Delta_1, \tag{26}$$

$$\frac{dF_1}{dz'}=-I_1\frac{1}{2\pi}\int_0^{2\pi}e^{i\theta}d\theta_0. \tag{27}$$

After introducing $\zeta=(I_1\mu_1)^{1/3}z'$, $\xi=\Delta_1/(I_1\mu_1)^{1/3}$, $\overline{\theta}=\theta+\xi\zeta$, and $F=[2\mu_1/(I_1\mu_1)^{2/3}]F_1e^{i\xi\zeta}$, Eqs. (25)–(27) yield

$$\frac{d^2\overline{\theta}}{d\zeta^2}=-\mathrm{Re}(Fe^{-i\overline{\theta}}), \tag{28}$$

$$\frac{dF}{d\zeta}-i\xi F=-\frac{1}{\pi}\int_0^{2\pi}e^{i\overline{\theta}}d\theta_0, \tag{29}$$

which is the simplest form of equations describing a one-dimensional, ''rigid-disk'' model of the conventional TWT with negligibly small space charge forces [22]. As follows from normalization of the variables in Eqs. (28) and (29), the factor $(I_1\mu_1)^{1/3}$ here plays the role of the Pierce gain parameter known in the theory of TWTs [23]. The boundary conditions for Eqs. (28) and (29) in the case of the TWT are $\theta=\theta_0$, $(d\theta/d\zeta)=0$, $F=F_0$ and, in the case of the twystron, $\theta=\theta_0-q\sin\theta_0$, $(d\theta/d\zeta)=0$, $F=0$.

Equations (28) and (29), as well as Eqs. (16)–(18), have the integral

$$4\frac{d\langle\theta\rangle}{d\zeta}=|F|^2-|F_0|^2, \tag{30}$$

which can be interpreted as the energy conservation law. In Eq. (30), $\langle\theta\rangle=(1/2\pi)\int_0^{2\pi}\overline{\theta}d\theta_0$ and at the entrance, $(d\langle\theta\rangle/d\zeta)|_0=0$. Again, introducing the normalized efficiency describing the electron bunching as

$$\hat{\eta}=\frac{d\langle\theta\rangle}{d\zeta}, \tag{31}$$

one can rewrite Eq. (30) as

$$|F|^2-|F_0|^2=4\hat{\eta}, \tag{32}$$

where the input wave intensity $|F_0|^2$ can usually be ignored. As follows from Eqs. (20), (26), and (31), the normalized efficiency $\hat{\eta}$ relates to the orbital efficiency $\eta_\perp$ as

$$\hat{\eta}=\frac{\mu_1}{(I_1\mu_1)^{1/3}}\eta_\perp. \tag{33}$$

So, at small values of I_1, the orbital $\eta_\perp$ and the total η electron efficiencies are small, even when the bunching described by $\hat{\eta}$ is efficient.

Equations (12)–(14), describing the excitation of backward waves in the regime of the dominant inertial bunching, can be reduced in the same way as was done with Eqs. (3)–(5), describing the forward wave interaction, to

$$\frac{d^2\bar{\theta}}{d\zeta^2} = -F_2'' e^{-i\bar{\bar{\theta}}}, \tag{34}$$

$$\frac{dF_2''}{d\zeta} - i\xi_2 F_2'' = iR\,\frac{1}{2\pi}\int_0^{2\pi} e^{i\bar{\bar{\theta}}}\bar{\theta}\, d\theta_0, \tag{35}$$

where

$$F_2'' = \frac{s_2}{(s_1 I_1)^{2/3}}\, F_2' e^{i\xi_2\zeta},$$

$$\bar{\bar{\theta}} = \frac{s_2}{s_1}\,\bar{\theta}$$

[here, $\xi_2 = \Delta_2/(I_1\mu_1)^{1/3}$], and where

$$R = \frac{s_2 I_2'}{s_1 I_1'} = \frac{s_2 I_2}{s_1 I_1}$$

is the ratio of normalized current parameters, which is proportional to the ratio of coupling parameters G of electrons to both waves [see Eqs. (10) and (11)]. For linear beam devices, this is the ratio of Pierce gain parameters: $R = C_2^3/C_1^3$.

III. EXCITATION OF BACKWARD WAVES IN LINEAR BEAM DEVICES

In this section, we present the results of the study of Eqs. (28), (29), and (31) describing the amplification of the forward wave and Eqs. (34) and (35) describing the excitation of backward waves in the presence of the forward wave in linear beam devices and in gyrodevices with dominant inertial bunching. For the TWT in Fig. 1(a), the contours of the equal normalized efficiency determined by Eq. (31) are shown by dashed lines in the plane of the parameters ''normalized length versus input wave amplitude.'' The detuning ξ is taken here to equal 1.5. At this value of ξ the normalized efficiency $\hat{\eta}$ is a little smaller than that for the optimal value ($\xi_{\rm opt} = 1.8$), however, the distance at which the peak efficiency is realized is much shorter. So, we choose this value of ξ since the stability of operation greatly improves as the interaction length shortens. Solid lines in this figure correspond to the starting length for backward wave excitation calculated for different ratios of the Pierce gain parameters R. As seen from Fig. 1(a), as this ratio decreases, the efficiency of stable amplification of the forward wave increases drastically. In Fig. 1(b), corresponding detunings ξ_2 as functions of the input wave amplitude are shown for different R's. The fact that the starting length for backward wave oscillations grows as the input wave amplitude increases demonstrates the nonlinear effect of suppression of these oscillations by the forward wave. A rapid increase in this length

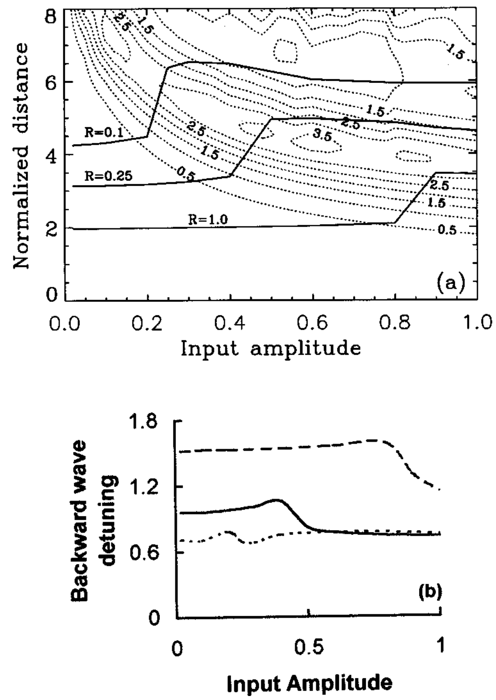

FIG. 1. (a) Contours of normalized efficiency of the forward wave operation in the TWT (dotted lines) and the starting length of backward wave excitation for different values of the ratio of Pierce gain parameters for the backward and forward waves, R (solid lines). (b) Normalized detuning of the backward wave ξ_2 in the TWT as a function of the input amplitude of the forward wave: dashed, solid, and dotted lines correspond to $R = 1.0$, 0.25, and 0.1, respectively.

occurring when solid curves pass the top of the hill formed by lines of equal efficiencies corresponds to the deformation of the axial structure of the backward wave. This evolution of the axial structure is shown in Fig. 2 and can be associated with electron overbunching in the field of the traveling wave, which occurs at too long distances. Coming back to Fig. 1(b), let us note, first, that the detuning ξ_2 determines the frequency of the backward wave, and second, that this detuning strongly depends on the ratio of Pierce gain parameters, R, and also on the input wave amplitude. In the absence of the forward wave, the starting length and the detuning ξ_2 for the backward wave coincide with those found in Ref. [21].

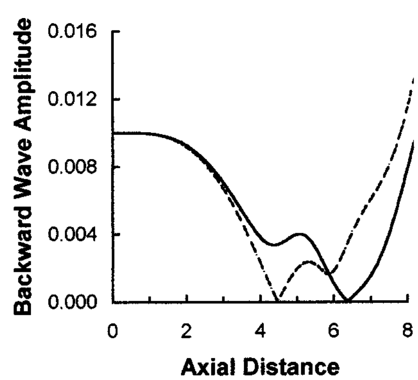

FIG. 2. Evolution of the backward wave axial structure with the increase in the input amplitude of the forward wave: dashed and solid lines correspond to $F_0 = 0.2$ and 0.25, respectively; $R = 0.1$.

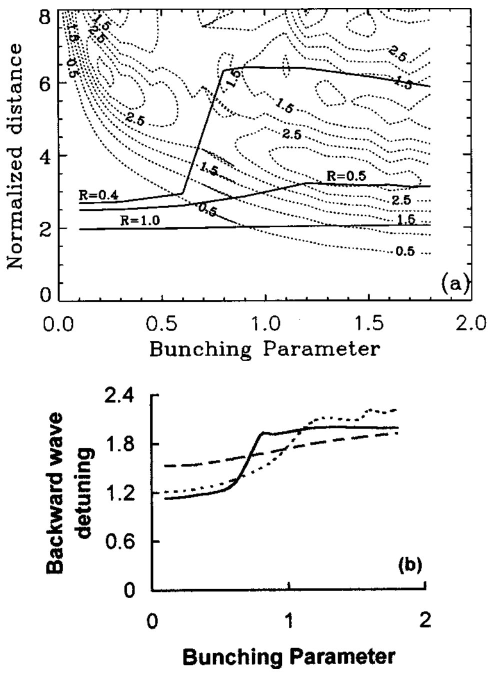

FIG. 3. (a) Contours of normalized efficiency of the forward wave operation in the twystron (dotted lines) and the starting length of backward wave excitation for different values of R (solid lines). (b) Normalized detuning of the backward wave ξ_2 in the twystron as a function of the bunching parameter q for several values of R.

For the twystron configuration the starting length for backward wave excitation is shown for several values of R in the plane of ''normalized length versus bunching parameters'' in Fig. 3(a), where also the contours of equal normalized efficiencies are shown by dashed lines. The detunings ξ_2 as functions of the bunching parameters are shown in Fig. 3(b). These figures are very similar qualitatively to Figs. 1(a) and 1(b); however, quantitatively, they are different: as follows from their comparison, the suppression effect in twystrons is better pronounced since the forward-wave, high-efficiency operation can be realized at larger values of R.

IV. EXCITATION OF BACKWARD WAVES IN GYRODEVICES

In this section, we present results of our studies of gyro-TWTs and gyrotwystrons. Recall that the forward wave operation of these devices is described by Eqs. (16)–(18) and (20) with corresponding boundary conditions, and the backward wave excitation is described by Eqs. (12)–(14).

The gyro-TWT was studied for a fixed value of the normalized beam current parameter $I_1'=0.05$, which is typical for some experimental conditions. The operation in forward waves and excitation of backward waves at the first and second cyclotron harmonics were studied. Figures 4(a), 4(b), and 4(c) illustrate the cases of, respectively, $s_1=s_2=1$; $s_1=1$, $s_2=2$; and $s_1=2$, $s_2=1$. For each value of the input wave amplitude F_0 the mismatch Δ_1' providing the maximum efficiency was chosen. Contours of equal values of the orbital efficiency $\eta_\perp$ are shown in these figures by dotted lines and the solid lines show starting conditions for backward waves at different values of the ratio of normalized beam current parameters I_2'/I_1'.

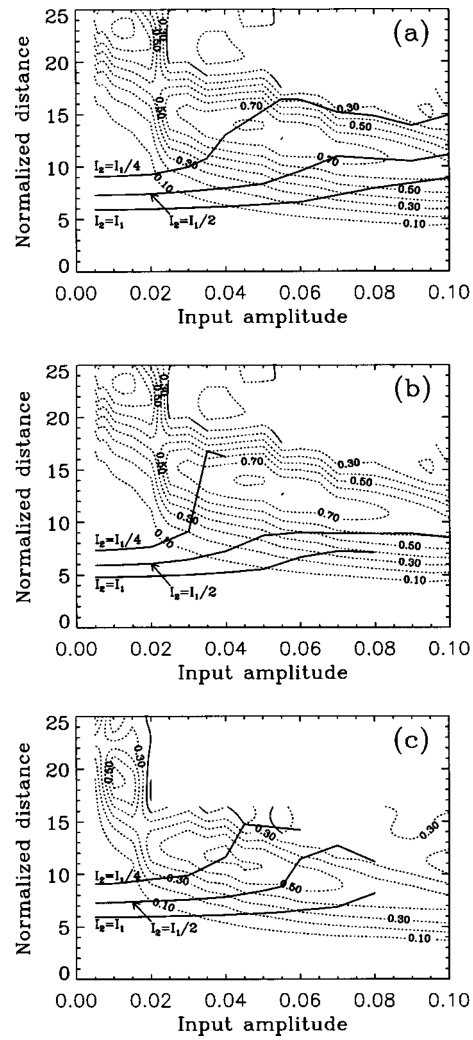

FIG. 4. (a) Contours of orbital efficiency of the forward wave operation in the gyro-TWT (dotted lines) and the starting length of backward wave excitation for different values of the ratio of normalized current parameters for these waves and for the waves' interaction with electrons at different cyclotron harmonics: (a) $s_1=s_2=1$, (b) $s_1=1$, $s_2=2$, and (c) $s_1=2$, $s_2=1$.

As follows from Fig. 4(a), to realize operation with the maximum efficiency when both competing waves are in the fundamental cyclotron resonance with electrons one should have a ratio of normalized currents about 1/4 or less. At larger ratios the maximum orbital efficiency (above 80%) cannot be realized; however, for any fixed value of the input wave amplitude in the range $0.04<F_0\leqslant 0.08$, the decrease in the ratio I_2'/I_1' gives a significant enhancement in the efficiency. When the forward wave is at the fundamental resonance with electrons while the backward wave is resonant with the second cyclotron harmonic [Fig. 4(b)], the maximum efficiency can be realized when the ratio of the normalized currents is about 1/3 or less. Again, at larger ratios the increase in the achievable efficiency with the decrease in the I_2'/I_1' ratio is very impressive, especially when this ratio is smaller than 1/2. The forward wave operation at the second harmonic, as follows from Fig. 4(c), is less efficient: the maximum orbital efficiency is higher than 60%. This maximum efficiency can be realized when for the competing backward waves, which can be excited at the fundamental

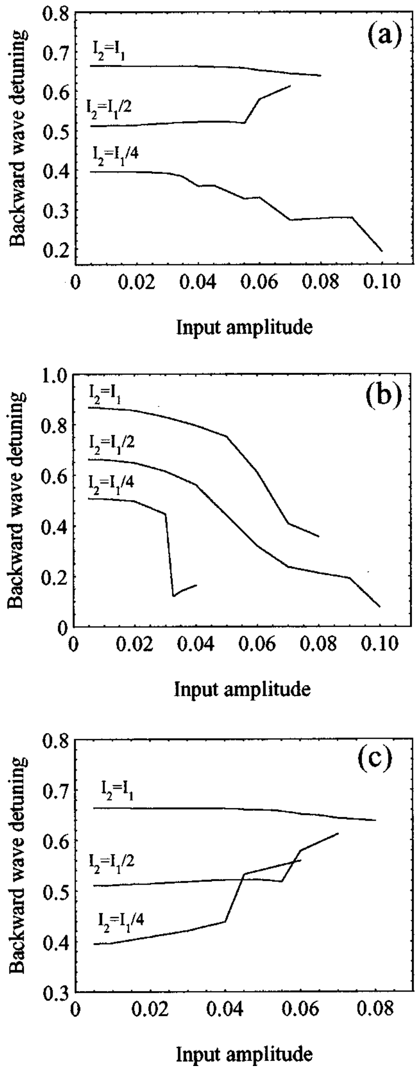

FIG. 5. Normalized detuning of the backward wave, Δ_2', in the gyro-TWT as a function of the input amplitude of the forward wave for several values of the ratio I_2'/I_1' and for the waves' interaction at different harmonics: (a) $s_1=s_2=1$, (b) $s_1=1$, $s_2=2$, and (c) $s_1=2$, $s_2=1$.

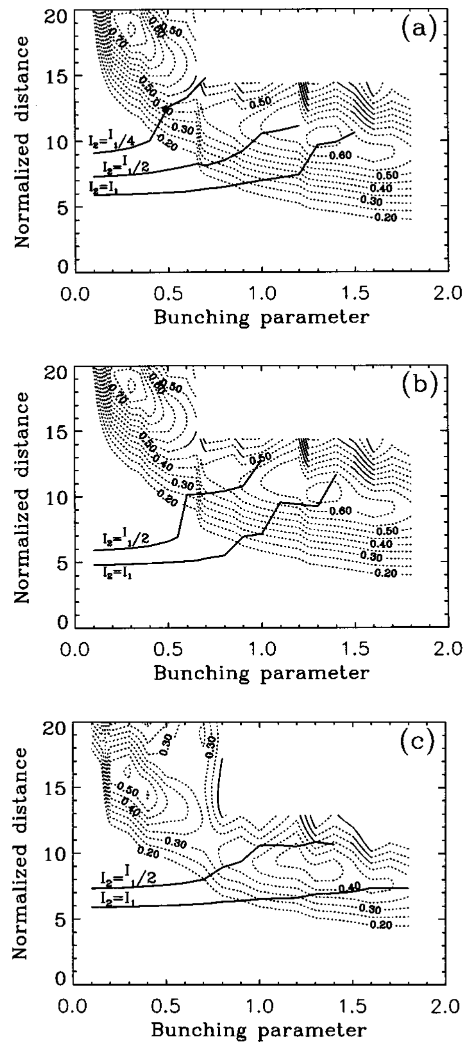

FIG. 6. Contours of orbital efficiency of the forward wave interaction in the gyrotwystron (dotted lines) and the starting length of backward wave excitation for several values of the ratio I_2'/I_1': (a) $s_1=s_2=1$, (b) $s_1=1$, $s_2=2$, and (c) $s_1=2$, $s_2=1$.

resonance, the ratio of the normalized currents I_2'/I_1' is about 1/4 or less.

The detunings Δ_2', which correspond to the backward wave self-excitation conditions, are shown in Figs. 5(a), 5(b), and 5(c), again corresponding, respectively, to the cases of $s_1=s_2=1$, $s_1=1$; $s_2=2$; and $s_1=2$, $s_2=1$.

Results of the study of gyrotwystrons are shown in Figs. 6 and 7, where the role of the input wave amplitude F_0 (for the gyro-TWT) is played now by the bunching parameter q. Here, the figures (a), (b), and (c) again correspond, respectively, to the cases of $s_1=s_2=1$; $s_1=1$, $s_2=2$; and $s_1=2$, $s_2=1$. The lowest peak in the orbital efficiency of the gyrotwystron operating at the fundamental and/or second cyclotron harmonic exceeds, respectively, 65% and 45%. In the case of operation at the fundamental harmonic this efficiency can be realized when the ratio of normalized currents is less than or equal to one, no matter whether the backward wave resonates at the first or second harmonic. In the case of the forward wave operation at the second harmonic, this ratio for the parasite at the fundamental should be smaller than approximately 3/4. These numbers, being compared with corresponding data shown above in Fig. 4, demonstrate that the gyrotwystron is less susceptible to excitation of parasitic backwards waves than the gyro-TWT. This feature of the gyrotwystron can be explained by the fact that at the entrance to the output waveguide of this device the beam can be well prebunched, while in the gyro-TWT, near the entrance, the effect of the small amplitude forward wave on the electron bunching can be rather weak, which cannot prevent the self-excitation of backward waves. (This explanation is also valid for the TWTs and twystrons considered in Sec. III.) The detunings Δ_2' shown as the functions of the bunching parameter q in Fig. 7 also exhibit the dependence, which in some cases is opposite to that shown in Fig. 5 for the gyro-TWT.

V. DISCUSSION

Let us briefly discuss how the results obtained can be applied to concrete microwave sources. Let us start from linear beam devices as a simpler case. The self-excitation conditions of parasitic backward waves here are determined

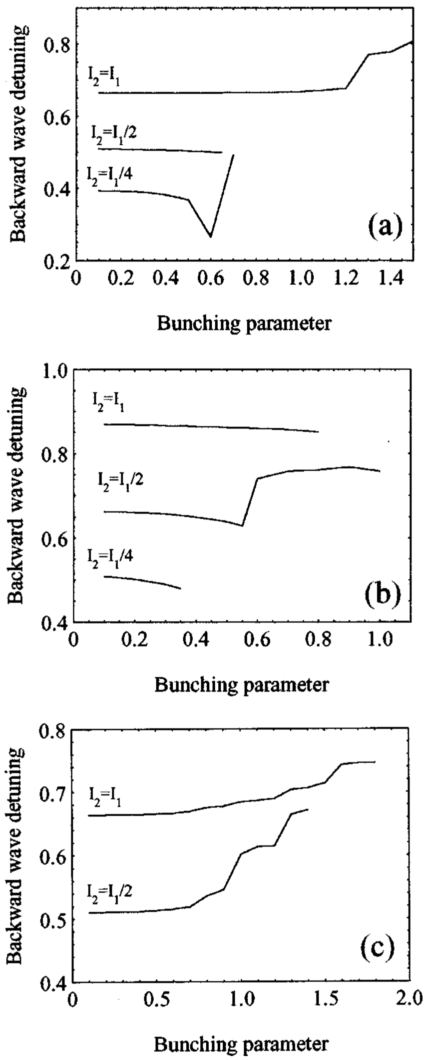

FIG. 7. Normalized detuning of the backward wave, Δ_2', in the gyrotwystron as a function of the bunching parameter: (a) $s_1=s_2=1$, (b) $s_1=1$, $s_2=2$, and (c) $s_1=2$, $s_2=1$.

by the ratio of Pierce gain parameters

$$R=C_2^3/C_1^3=K_2/K_1,$$

where K_1 and K_2 are the coupling impedances of an electron beam to the forward and backward waves, respectively. Introducing the functions $\Psi(r)$ and $\Phi_{1,2}(r)$ for describing, respectively, the transverse structure of the beam current density and transverse structures of the forward (Φ_1) and backward (Φ_2) waves, one can readily derive (cf. Refs. [22, 23]) that the ratio K_2/K_1 is proportional to

$$\frac{k_{1,z}}{k_{2,z}}\frac{\left(\int_{S_b}\Psi\Phi_2 ds_\perp\right)^2}{\left(\int_{S_b}\Psi\Phi_1 ds_\perp\right)^2}, \tag{36}$$

where S_b is the beam cross section. So, by choosing the radial profile of the beam properly, one can decrease this ratio when the waves have different transverse structures. Axial wave numbers in Eq. (36) can be defined in a zero order approximation by intersection of the electron beam dispersion line $\omega=k_z v_z$ with the dispersion curves of some specific waves in a given slow wave structure. In the first order approximation, one should use instead of $\omega=k_z v_z$ the values ξ and ξ_2 found above, which characterize the detunings from the exact synchronism between electrons and the waves. Recall that for a forward wave operating in the regime of convective instability the frequency is given by the driver, so the detuning ξ determines the axial wave number $k_{1,z}$. On the contrary, for a backward wave excited due to the absolute instability the detuning ξ_2 determines the frequency of oscillations; a corresponding axial wave number should be found from the dispersion curve.

In the case of gyrodevices, the competing waves can be in cyclotron resonance with electrons at different cyclotron harmonics. Consider, as an example, the experiment described in Ref. [8] where the competition between the forward TE_{11} wave operating at the fundamental cyclotron resonance and parasitic backward TE_{21} wave excited at the second cyclotron harmonic was studied. Recall that in this experiment an electron beam with an orbital to axial velocity ratio $\alpha\simeq 1$, voltage of up to 95 kV and current of up to $2A$ amplified the circularly polarized TE_{11} wave in a waveguide with a 0.2654 cm radius and 17.5 cm length. A 34.712-GHz frequency of operation was set by a fixed frequency magnetron driver and the input power was varied from 5 W to about 1.5 kW. The external magnetic field was in the range of 12.5 kG. The parasitic oscillations were observed at about 56.8 GHz and were associated with the backward wave excitation of the TE_{21} wave at the second cyclotron harmonic.

These frequencies and the waveguide radius mentioned above yield normalized axial wave numbers of about 0.3 and 0.25 for the first and second waves, respectively. The normalized length of the interaction region is slightly above 20 and the normalized detuning Δ_1' for a given magnetic field is equal to 0.49, which is close to the optimal values found in our and previous calculations [15–17]. To determine normalized beam current parameters I_1' and I_2', it was necessary to assume a certain guiding center radius of electrons since this radius was not specified in Ref. [8]. We assumed $R_0=1$ mm, which yielded for the coupling parameters determined by Eq. (11), $G_{11}\simeq 0.96$ and $G_{21}\simeq 0.4$ for the TE_{11} and TE_{21} waves, respectively. The ratio R of normalized current parameters for this beam radius is close to 0.18. The normalized current parameter of the operating TE_{11} wave, I_1', for the maximum current is equal to 0.062, but in a typical range of voltages (near 90 kV) and currents (about 1 A), I_1' is in the range of 0.02–0.04. (Recall that the results shown in Fig. 4 correspond to $I_1'=0.05$.) The initial value of the normalized wave amplitude, as follows from the expressions given elsewhere [24], for a drive power of 5 W to 1.5 kW is in the range of 0.0015 to 0.027.

So, the result, which is the closest to the experimental data given in Ref. [8], is the curve shown in Fig. 4(b) for $R=0.25$, which demonstrates a significant suppression of the parasitic wave when the normalized input amplitude of the operating wave exceeds 0.03. It is obvious that at smaller R's this effect should appear at smaller F_0's. Therefore, the experimental evidence of the suppression of parasitic waves with $R=0.18$ at the drive power exceeding 1 kW (which corresponds to $F_0\leqslant 0.02$) looks consistent with the results of our calculations.

VI. CONCLUSION

The theory is developed that allows one to study the self-excitation conditions of backward waves in forward-wave amplifiers operating in a large signal regime. Such devices as traveling wave tubes and twystrons driven either by linear electron beams or the beams of gyrating electrons are considered. The effect of nonlinear suppression of parasitic backward waves by forward waves operating in the large signal regime is demonstrated. The formalism developed and the results obtained can be applied to a wide class of forward wave amplifiers.

The goal of the present paper was to develop a general formalism that allows one to study the problem of stable operation in forward-wave amplifiers and to illustrate this theory by a number of simple examples. The formalism can easily be generalized further for including the effects of electron velocity spread, distributed wall losses, and other factors important for operation of real devices.

ACKNOWLEDGMENTS

This work has been supported by the DOD MURI program under AFOSR Grant No. F4962001528306 and by the Naval Research Laboratory.

APPENDIX: DERIVATION OF EQUATIONS DESCRIBING THE EXCITATION OF BACKWARD WAVES IN THE PRESENCE OF FORWARD WAVES IN GYRO-TWAs

The external magnetic field $\mathbf{H}_0$ required for the cyclotron resonance is usually much larger than electromagnetic (EM) fields generated by electron beams. Therefore, the effect of EM fields on electron motion can be treated as a small perturbation in electron gyration. Introducing the gyrophase as $\Theta=\int_0^\tau \Omega\, d\tau' + \varphi$, where Ω is the energy-dependent electron cyclotron frequency, and components of electron momentum as $p_x = p_\perp \sin\Theta$, $p_y = p_\perp \cos\Theta$, p_z, one can derive from Eq. (2) the following equations for perturbations in $p_\perp$, φ, and p_z [14–16]

$$\frac{dp'_\perp}{dz'}=\mathcal{F}_\theta, \quad p'_\perp \frac{d\varphi}{dz'}=-\mathcal{F}_r, \quad \frac{dp'_z}{dz'}=\mathcal{F}_z. \tag{A1}$$

Here, the normalized Lorentz force, $\vec{\mathcal{F}}$, acting on electrons is given by the right-hand side of Eq. (2). If we represent $p'_\perp$, φ, and p'_z as $p'_\perp = p'_{\perp(0)} + \tilde{p}_\perp$, $\varphi=\varphi_{(0)}+\tilde{\varphi}$, and $p'_z = p'_{z(0)} + p'_z$ (also, $\gamma=\gamma_{(0)}+\tilde{\gamma}$), where the subscript "(0)" denotes the motion in the absence of the backward wave but in the presence of the forward one), then for perturbations caused by the backward wave we get from Eq. (A1)

$$\frac{d\tilde{p}_\perp}{dz'}=\mathcal{F}_{2,\theta}, \quad p'_{\perp(0)} \frac{d\tilde{\varphi}}{dz'}=-\mathcal{F}_{2,r}, \quad \frac{d\tilde{p}_z}{dz'}=\mathcal{F}_{2,z}. \tag{A2}$$

Here, the index "2" refers to the backward wave. In the reference frame whose center coincides with an electron guiding center, the Lorentz force is a periodic function of the cyclic polar coordinate Θ. Therefore, this force can be expanded as a sum of angular harmonics, among which, under the cyclotron resonance condition, only one is slowly variable with respect to the wave. So, after averaging over fast gyrations one can derive for the components of $\vec{\mathcal{F}}_2$ the following equations (cf. Refs. [15,16]):

$$\mathcal{F}_{2,\theta}=p_{\perp 0}\,\frac{(1-u)^{(s_2-1)/2}}{1-bu}\,\mathrm{Re}\{F_2 e^{-i(\theta_{2(0)}-\varphi_2)}\}, \tag{A3}$$

$$\mathcal{F}_{2,r}=p_{\perp 0}\,\frac{(1-u)^{(s_2-1)/2}}{1-bu}\,\mathrm{Re}\{iF_2 e^{-i(\theta_{2(0)}-\varphi_2)}\}, \tag{A4}$$

$$\mathcal{F}_{2,z}=-\frac{h_2\gamma_0\beta_{\perp 0}^2}{1+h_2\beta_{z0}}\,\frac{(1-u)^{s_2/2}}{1-bu}\,\mathrm{Re}\{F_2 e^{-i(\theta_{2(0)}-\varphi_2)}\}, \tag{A5}$$

Note that, since we assume that the amplitude of the backward wave is much smaller than the amplitude of the forward waves, Eqs. (A3)–(A5) do not contain perturbations in electron motion caused by the backward wave. This means that u is determined by Eq. (3) and the slowly variable phase of the resonant harmonic of electron gyrations with respect to the phase of the backward wave,

$$\theta_2=s_2\Theta-(\omega_2 t+k_{2,z}z),$$

is represented as $\theta_{2(0)}+\tilde{\theta}$ and in the right-hand side of Eqs. (A3)–(A5) the perturbation $\tilde{\theta}$ is ignored. The phase $\underline{\theta_2} = \theta_{2(0)}-\varphi_2$, which is present in Eqs. (A3)–(A5), can be expressed via θ determined by Eq. (4) as

$$\bar{\theta}_2=\frac{s_2}{s_1}\,\theta+\frac{s_1 m_2 - s_2 m_1}{s_1}\,\psi+\frac{s_2\omega_1-s_1\omega_2}{s_1}\,t, \tag{A6}$$

where ψ is the azimuthal coordinate of the electron guiding center.

In accordance with Eq. (A6), one can derive for the phase $\bar{\theta}_2$ an equation similar to Eq. (4) for θ:

$$\frac{d\bar{\theta}_2}{dz'}=\frac{1}{1-bu}\,\{\mu_2 u-\Delta_2+s_2(1-u)^{(s_1/2)-1}\,\mathrm{Im}(F_1 e^{-i\theta})\}, \tag{A7}$$

where

$$\mu_2=\frac{s_2\beta_{\perp 0}^2(1+h_1h_2)}{2\beta_{z0}(1+h_2\beta_{z0})(1-h_1\beta_{z0})},$$

and

$$\Delta_2=s_2\,\frac{1+h_2\beta_{z0}-s_2\Omega_0/\omega_2}{\beta_{z0}(1+h_2\beta_{z0})}$$

is the normalized cyclotron resonance mismatch for the backward wave. Note that the presence of both axial wave numbers in the parameter μ_2 reflects the fact that we consider the changes in the gyrophase, which are caused by the forward wave, with respect to the phase of the backward wave. As follows from Eq. (A6), the boundary condition for $\bar{\theta}_2$ can be written as

$$\overline{\theta}_2(0)=\frac{s_2}{s_1}\,\theta(0)+\overline{\psi},$$

$$\text{where}\quad \overline{\psi}=\frac{s_1m_2-s_2m_1}{s_1}\,\psi+\frac{s_2\omega_1-s_1\omega_2}{s_1}\,t_0. \tag{A8}$$

The normalized backward wave amplitude F_2 in Eqs. (A3)–(A5) is equal to

$$\frac{1+h_2\beta_{z0}}{\kappa_2\gamma_0\beta_{\perp0}\beta_{z0}}\left[\frac{1}{(s_2-1!)2^{s_2}}\left(\frac{s_2\kappa_2\beta_{\perp0}}{1+h_2\beta_{z0}}\right)^{s_2-1}\right]\frac{eA_2}{m_0c\Omega_0}\,|L_2|. \tag{A9}$$

Here, h_2 and κ_2 are, respectively, the axial and transverse backward wave numbers normalized to ω_2/c; the value of h_2 is positive, thus $1+h_2\beta_{z0}\approx s_2\Omega_0/\omega_2$ corresponds to the Doppler frequency down shifted operation in the backward wave. Note that, as follows from the equation for $\tilde{p}_z$ given in Eq. (A2) and the equation for perturbations in electron normalized energy $\tilde{\gamma}$, which can be easily derived, these perturbations are related as

$$\tilde{p}_z=-h_2\tilde{\gamma}. \tag{A10}$$

Equation (A10) corresponds to the autoresonance integral for the case of electron interaction with the backward wave [15], $p_zc+h_2\mathcal{E}=\text{const}$, which shows that an electron radiating backward waves increases its axial momentum while losing the orbital one.

Using Eq. (A10) and the general relation between the normalized electron energy and momentum, $\gamma^2=1+p_z'^2+p_\perp'^2$, one can readily express perturbations in $\tilde{p}_\perp(p_\perp'=p_{\perp(0)}'+\tilde{p}_\perp)$ via $\tilde{\gamma}$:

$$\tilde{p}_\perp=\frac{1}{\beta_{\perp0}\sqrt{1-u}}\left[1+h_2\beta_{z0}-(1+h_1h_2)\,\frac{\gamma_0-\gamma_{(0)}}{\gamma_0}\right]\tilde{\gamma}. \tag{A11}$$

When the changes in electron energy are small, $|\gamma_0-\gamma_{(0)}|\ll\gamma_0$, Eq. (A11) reduces to

$$\tilde{p}_\perp=\frac{1+h_2\beta_{z0}}{\beta_{\perp0}\sqrt{1-u}}\,\tilde{\gamma}. \tag{A12}$$

Introducing normalized perturbations $\hat{p}_\perp=\tilde{p}_\perp/p_{\perp0}$, $\hat{p}_z=\tilde{p}_z/p_{z0}$, one can derive for $\hat{p}$ from Eqs. (A2) and (A3)

$$\frac{d\hat{p}_\perp}{dz'}=\frac{(1-u)^{(s_2-1)/2}}{1-bu}\,\mathrm{Re}(F_2e^{-i\overline{\theta}_2}), \tag{A13}$$

and express $\hat{p}_z$ via $\hat{p}_\perp$ as

$$\hat{p}_z=-2b_2\sqrt{1-u}\,\hat{p}_\perp. \tag{A14}$$

Here $b_2=h_2\beta_{\perp0}^2/2\beta_{z0}(1+h_2\beta_{z0})$ is the recoil parameter for the backward wave.

The equation for the perturbation in the phase θ_2 (denoted as $\tilde{\theta}$) follows from Eqs. (A2), (A4), and (A7) and yields

$$\frac{d\tilde{\theta}}{dz'}=\frac{1}{1-bu}\left\{-\left[\frac{s_2(1-h_2^2)}{\beta_{z0}(1+h_2\beta_{z0})}-\frac{h_2}{\beta_{z0}(1-bu)}\times(\Delta_2-\mu_2u)\right]\tilde{\gamma}+s_2(1-u)^{(s_2/2)-1}\,\mathrm{Im}(F_2e^{-i\overline{\theta}_2})\right\}. \tag{A15}$$

Equations (A11)–(A15) describe perturbations in the electron motion due to the field of a small amplitude backward wave. The equation describing the excitation of this wave can be derived from Maxwell's equations by using the method described elsewhere [4,14,15], which yields

$$\frac{dF_2}{dz'}=I_2\,\frac{1}{2\pi}\int_0^{2\pi}\frac{(1-u)^{s_2/2}}{1-bu}\,e^{i\overline{\theta}_2}\times\left[\frac{\hat{p}_\perp}{\sqrt{1-u}}-\frac{\hat{p}_z}{1-bu}+\frac{s_2-1}{2}\,\frac{\tilde{u}}{1-u}+i\tilde{\theta}\right]d\theta_0d\overline{\theta}_{20}. \tag{A16}$$

Here the perturbation in u ($\tilde{u}$) relates to the perturbation in γ ($\tilde{\gamma}$) present in Eqs. (A11) and (A12) as $\tilde{u}=2(1-h\beta_{z0})\tilde{\gamma}/\beta_{\perp0}^2\gamma_0$; the averaging over $\overline{\theta}_{20}$, which, as follows from Eq. (A8), is identical to the averaging over $\overline{\psi}$, corresponds either to the averaging over the azimuthal distribution of electron guiding centers when azimuthal indices of the forward and backward waves obey the condition

$$s_1m_2\neq s_2m_1, \tag{A17}$$

or to averaging over the period of beating $|2\pi s_2/(s_2\omega_1-s_1\omega_2)|$ if the condition (A17) is not fulfilled. The normalized current parameter I_2 for the backward wave has the same form as I_1 for the forward wave given by Eq. (10) (after corresponding changes in s, h, κ, and G).

Since Eqs. (A12)–(A16) are linearized with respect to perturbations caused by the backward wave, one can introduce, as was done in Ref. [9], perturbations averaged over the phase $\overline{\psi}$:

$$\overline{p_\perp}=\frac{1}{2\pi}\int_0^{2\pi}\hat{p}_\perp e^{i\overline{\psi}}d\overline{\psi}, \tag{A18a}$$

$$\overline{p_z}=\frac{1}{2\pi}\int_0^{2\pi}\hat{p}_z e^{i\overline{\psi}}d\overline{\psi}, \tag{A18b}$$

$$\overline{u}=\frac{1}{2\pi}\int_0^{2\pi}\tilde{u}_z e^{i\overline{\psi}}d\overline{\psi}, \tag{A18c}$$

$$\overline{\theta}=\frac{1}{2\pi}\int_0^{2\pi}\tilde{\theta}e^{i\overline{\psi}}d\overline{\psi}. \tag{A18d}$$

In these variables, Eqs. (A12)–(A16) yield

$$\frac{d\overline{p_\perp}}{dz'}=\frac{(1-u)^{(s_2-1)/2}}{1-bu}\,\frac{1}{2}\,F_2e^{-i\overline{\overline{\theta}}_2}, \tag{A19}$$

$$\overline{p_z}=-2b_2\sqrt{1-u}\,\overline{p_\perp}, \tag{A20}$$

$$\bar{u}=2\,\frac{1-h\beta_{z0}}{1+h_2\beta_{z0}}\,\sqrt{1-u}\,\bar{p}_\perp\,, \tag{A21}$$

$$\frac{d\bar{\theta}}{dz'}=\frac{1}{1-bu}\left\{-\left[\frac{s_2(1-h_2^2)}{\beta_{z0}(1+h_2\beta_{z0})}-\frac{h_2}{\beta_{z0}(1-bu)}\right.\right.$$
$$\left.\times(\Delta_2-\mu_2 u)\right]\frac{\beta_{\perp 0}^2}{2(1-h\beta_{z0})}\,\bar{u}-i\,\frac{s_2}{2}$$
$$\left.\times(1-u)^{(s_2/2)-1}F_2 e^{-i\bar{\bar{\theta}}_2}\right\}, \tag{A22}$$

$$\frac{dF_2}{dz'}=I_2\,\frac{1}{2\pi}\int_0^{2\pi}\frac{(1-u)^{s_2/2}}{1-bu}\,e^{i\bar{\bar{\theta}}_2}\left[\frac{\bar{p}_\perp}{\sqrt{1-u}}-\frac{\bar{p}_z}{1-bu}\right.$$
$$\left.+\frac{s_2-1}{2}\,\frac{\bar{u}}{1-u}+i\bar{\theta}\right]d\theta_0. \tag{A23}$$

Here, in accordance with Eqs. (A6) and (A8), $\bar{\bar{\theta}}_2=\bar{\theta}_2-\bar{\psi}$. The phase $\bar{\bar{\theta}}_2$ is determined by the same equation [Eq. (A7)] as the phase θ_2. Certainly, the elimination of distribution in ψ allows one to significantly shorten the computer time required for calculations.

Below, we will consider the excitation of both waves at frequencies close to cutoff when b, $b_2\rightarrow 0$, and $h\beta_{z0}$, $h_2\beta_{z0}\ll 1$. Then Eqs. (A19)–(A23) are reduced to

$$\frac{d\bar{p}}{dz'}=\frac{1}{2}\,(1-u)^{(s_2-1)/2}F_2'' e^{-i\bar{\bar{\theta}}}, \tag{A24}$$

$$\bar{p}_z=0,\quad \bar{u}=2\sqrt{1-u}\,\bar{p}_\perp\,, \tag{A25}$$

$$\frac{d\bar{\theta}}{dz'}=-2\mu_2\sqrt{1-u}\,\bar{p}_\perp-i\,\frac{s_2}{2}\,(1-u)^{s_2/2}F_2'' e^{-i\bar{\bar{\theta}}}, \tag{A26}$$

$$\frac{dF_2}{dz'}-i\Delta_2 F_2''=I_2\,\frac{1}{2\pi}\int_0^{2\pi}(1-u)^{s_2/2}e^{i\bar{\bar{\theta}}}$$
$$\times\left[\frac{s_2}{\sqrt{1-u}}\,\bar{p}_\perp+i\bar{\theta}\right]d\theta_0, \tag{A27}$$

where $\bar{\bar{\theta}}=\bar{\bar{\theta}}_2-\Delta_2 z'$, $F_2''=F_2 e^{i\Delta_2 z'}$, and $\mu_2=s_2\beta_{\perp 0}^2/2\beta_{z0}$. This parameter μ_2 can be eliminated from Eqs. (A24)–(A27) by introducing

$$\zeta'=\frac{\beta_{\perp 0}^2}{2\beta_{z0}}\,z',\quad F_2'=\frac{2\beta_{z0}}{\beta_{\perp 0}^2}\,F_2,\quad I_2'=\left(\frac{2\beta_{z0}}{\beta_{\perp 0}^2}\right)^2 I_2,$$

which yield

$$\frac{d\bar{p}_\perp}{d\zeta'}=\frac{1}{2}\,(1-u)^{(s_2-1)/2}F_2' e^{-i\bar{\bar{\theta}}}, \tag{A28}$$

$$\frac{d\bar{\theta}}{d\zeta'}=-2s_2\sqrt{1-u}\,\bar{p}_\perp-i\,\frac{s_2}{2}\,(1-u)^{(s_2/2)-1}F_2 e^{-i\bar{\bar{\theta}}}, \tag{A29}$$

$$\frac{dF_2'}{d\zeta'}-i\Delta_2 F_2'=I_2'\,\frac{1}{2\pi}\int_0^{2\pi}(1-u)^{s_2/2}e^{i\bar{\bar{\theta}}}$$
$$\times\left[\frac{s_2}{\sqrt{1-u}}\,\bar{p}_\perp+i\bar{\theta}\right]d\theta_0, \tag{A30}$$

[1] A. S. Gilmour, Jr., *Microwave Tubes* (Artech House, Norwood, MA, 1986), Chaps. 10, 11.
[2] J. L. Hirshfield and V. L. Granatstein, IEEE Trans. Microwave Theory Tech. **25**, 522 (1977).
[3] T. C. Marshall, *Free-Electron Lasers* (MacMillan, New York, 1985).
[4] V. A. Flyagin, A. V. Gaponov, M. I. Petelin, and V. K. Yulpatov, IEEE Trans. Microwave Theory Tech. **25**, 514 (1977).
[5] Y. Y. Lau, K. R. Chu, L. Barnett, and V. L. Granatstein, Int. J. Infrared Millim. Waves **2**, 395 (1981); V. L. Bratman and G. G. Denisov, Int. J. Electron. **72**, 969 (1992).
[6] K. R. Chu, L. R. Barnett, W. K. Lau, L. H. Chang, A. T. Lin, and C. C. Lin, Phys. Fluids B **3**, 2403 (1991).
[7] K. R. Chu, L. R. Barnett, H. Y. Chen, S. H. Chen, Ch. Wang, Y. S. Yeh, Y. C. Tsai, T. T. Yang, and T. Y. Dawn, Phys. Rev. Lett. **74**, 1103 (1995).
[8] L. R. Barnett, L. H. Chang, H. Y. Chen, K. R. Chu, W. K. Lau, and C. C. Tu, Phys. Rev. Lett. **63**, 1062 (1989).
[9] G. S. Nusinovich, Int. J. Electron. **51**, 457 (1981); see also, I. G. Zarnitsyna and G. S. Nusinovich, Radiophys. Quantum Electron. **17**, 1418 (1974).
[10] G. P. Saraph, T. M. Antonsen, Jr., B. Levush, and G. I. Lin, IEEE Trans. Plasma Sci. **20**, 115 (1992).
[11] K. R. Chu and A. T. Lin, IEEE Trans. Plasma Sci. **16**, 90 (1988).
[12] P. E. Latham and G. S. Nusinovich, Phys. Plasmas **2**, 3494 (1995); **2**, 3511 (1995).
[13] N. M. Kroll, in *Novel Sources of Coherent Radiation*, Physics of Quantum Electronics, Vol. 5, edited by S. F. Jackobs, M. Sargent III, and M. O. Scully (Addison-Wesley, Reading, MA, 1978), p. 115; see also V. L. Bratman, N. S. Ginzburg, and M. I. Petelin, Opt. Commun. **30**, 409 (1979); A. Gover and P. A. Spangle, IEEE Trans. Quantum Electron. **17**, 1196 (1981).
[14] V. K. Yulpatov, Izv. Vuzov, Radiofiz. **10**, 846 (1967) [Sov. Radiophys. **10**, 471 (1967)].
[15] N. S. Ginzburg, I. G. Zarnitsyna, and G. S. Nusinovich, Radiotekh. Elektron. **24**, 1146 (1979) [Radio Eng. Electron. Phys. **24**, 113 (1979)].
[16] A. W. Fliflet, Int. J. Electron. **61**, 1049 (1986).
[17] G. S. Nusinovich and H. Li, Int. J. Electron. **72**, 895 (1992).
[18] M. I. Petelin and V. K. Yulpatov, Izv. Vuzov., Radiofiz. **18**, 290 (1975) [Sov. Radiophys. **18**, 212 (1975)].
[19] G. S. Nusinovich, B. Levush, and O. Dumbrajs, Phys. Plasmas **3**, 3133 (1996).
[20] M. A. Moiseev, G. S. Nusinovich, Izv. Vuzov., Radiofiz. **17**, 1709 (1974) [Sov. Radiophys. **17**, 1305 (1974)].

[21] L. R. Walker, J. Appl. Phys. **24**, 854 (1953); see also H. R. Johnson, Proc. IRE **43**, 684 (1955).
[22] L. A. Vainshtein, Radiotekh. Elektron. **2**, 883 (1957) [Radio Eng. Electron. Phys. **2**, 92 (1957)]; see also, J. E. Rowe, *Nonlinear Electron-Wave Interaction Phenomena* (Academic Press, New York, 1965), Chap. VI.
[23] J. R. Pierce, *Traveling Wave Tubes* (Van Nostrand, New York, 1950).
[24] G. S. Nusinovich and M. Walter, Phys. Plasmas **4**, 3394 (1997).